

spectroscopic studies of their excited states are being carried out. Synthesis of bipyridinium acceptor molecules in zeolites and their spectroscopic properties are being examined. The ruthenium molecular assembly is being coupled with the acceptor/donor derived zeolites and examination of the dynamics of light-driven electron/hole transfer is being studied. Practical demonstration of charge propagation and long-range spatial separation using zeolite membranes has been demonstrated.

Progress Report :

I. Zeolite Membrane Development :

We have developed optimized methods for growth of zeolite A and Y membranes. Using zeolite Y, we have made seed layer coatings that are crack- and agglomerate-free, by dip-coating from stable dispersions of nanocrystalline zeolites. Surface charge and colloidal charge stabilization were optimized by adjusting the pH to 11.5 at a low ionic strength. The optimum pH was established with zeta-potential measurements of the dispersion. The excellent homogeneity and $<1 \mu\text{m}$ thickness of the seed layers makes it possible to coat large areas.

Continuous, thin, oriented zeolite A membranes have been produced by a two-step synthesis on macroporous α -alumina supports. In the *first step*, zeolite A nano-cubes with ~ 350 nm edges are attracted to a cationic polymer having selective affinity for zeolite A and results in selective, dense-packed deposition of aligned zeolite A cubes. In a *second step* of hydrothermal epitaxial growth, the seed layer grows epitaxially into a continuous, meso-defect free, $\sim 1 \mu\text{m}$ thick zeolite A layer.

Current focus is on growth of oriented zeolite L membranes. Partially oriented zeolite L membranes were grown from disk-shaped zeolite L crystals to 2-7 micron thick membranes. For the synthesis of sub-micron sized membranes, seed crystals from 20-60 nanometers were used. However, complete orientation of the zeolite L membrane was not achieved, as required in Scheme 1. We are examining the strategy shown in Figure 1 for orientation with encouraging preliminary results as shown by the diffraction pattern. Flat-disk zeolite L crystallites were oriented onto the surface of a thin silica layer deposited on top of an optically smooth porous alumina support. A mesoporous silica layer (200-400 nm thick) was dip-coated onto macroporous alumina supports, followed by modification of the silica surface with a silane coupling agent, 3-chloropropyltrimethoxysilane. The bi-functionality of this coupling agent was utilized to covalently link zeolite L to the support surface, thus creating an oriented zeolite L seed layer.

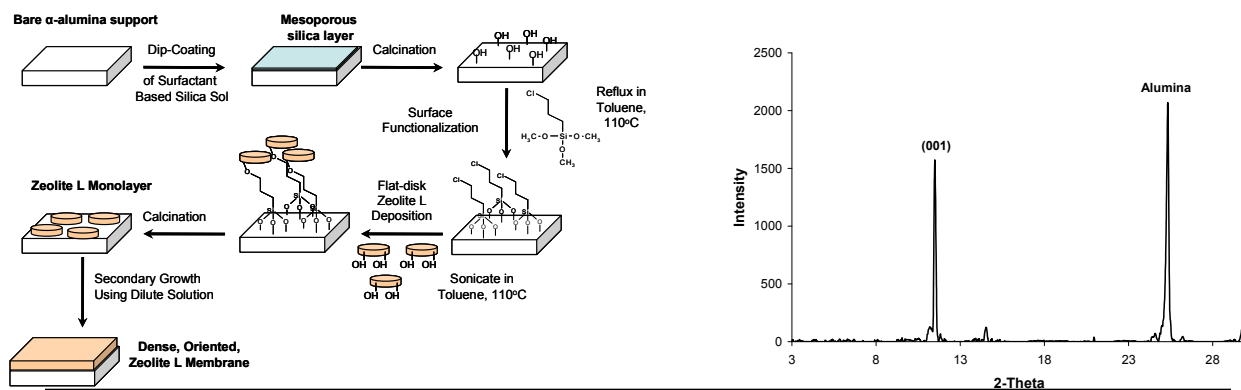
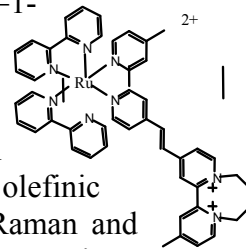


Figure 1. Left: Schematic of growing oriented zeolite L membranes. Right: XRD of seed layer deposition

Photosensitizer Development

Two ruthenium polypyridyl compounds of structural formula $[(bpy)_2RuL]^{2+}$ and $[(bpy)_2RuL_{DQ}]^{4+}$ (where bpy = bipyridine, L = 1, 2-bis[4-(4'-methyl)-2,2'-bipyridyl] ethene, L_{DQ} = 1-[4-(4'-methyl)-2,2'-bipyridyl]-2-[4-(4'-N,N'-tetramethylene-2,2'-bipyridinium)] ethene) have been synthesized and characterized. Photolysis of $[(bpy)_2Ru^{(II)}L]$ complex in solutions at pH 7 and 12 led to formation of species with increased emission quantum yields, ~ 55 nm blue-shift of the emission maximum to 625 nm and disappearance of the absorption band at 330 nm, the latter arising from the olefinic bond of the L ligand. With the help of chromatography, mass spectroscopy, Raman and NMR, it was found that the major photoproduct is a dimer of $[(bpy)_2Ru^{(II)}L]$. Photoreactions do not occur in the dark or in the aprotic solvent. We proposed that a Ru(III) radical intermediate is formed by photoinduced excited-state electron and proton transfer, which initiates the dimerization and can also undergo photochemical degradation.



On the other hand, the emission intensity and lifetime of $[(bpy)_2RuL_{DQ}]^{4+}$ is strongly quenched ($> 95\%$) compared to that of the $[(bpy)_2RuL]^{2+}$ complex. This quenching is attributed to the intramolecular electron transfer from the Ru center to the diaquat (DQ) moiety across the double bond of the L_{DQ} ligand. The $[(bpy)_2RuL_{DQ}]^{4+}$ complex exhibits strong stability towards visible light due to the presence of this electron acceptor DQ. We have chosen to work with $[(bpy)_2RuL_{DQ}]^{4+}$ as the photosensitizer of choice for attaching to the zeolite membrane surface.

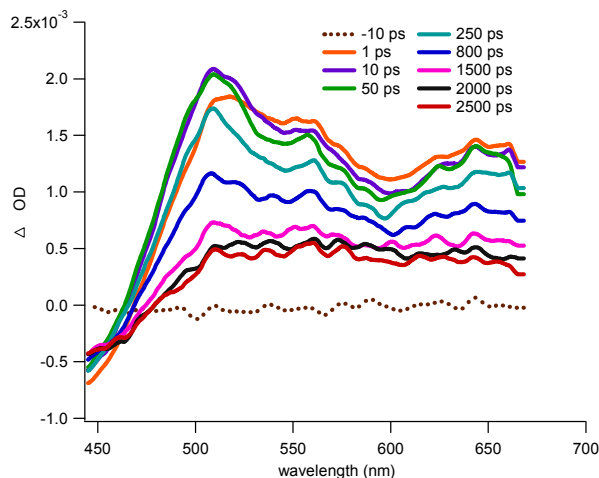


Figure 2. Broadband transient absorption of $[(bpy)_2RuLDQ]^{4+}$ excited at 400 nm with multiple transient spectra.

III. Transient Spectroscopic Studies:

Transient absorption spectra for the $[(bpy)_2RuL_{DQ}]^{4+}$ photosensitizer in acetonitrile are shown in Figure 2. The rich dynamics reflect the ultrafast decay of the initial MLCT state, charge trapping on the diaquat end of the L_{DQ} ligand, and eventual charge recombination. The signals indicate that charge is efficiently transported to the L_{DQ} ligand, where it is ready to be transferred to an electron acceptor located within the zeolite framework. We have also studied the excited state dynamics of methyl viologen encapsulated in zeolite nanocrystals. Significant differences are observed compared

to bulk solution. Our measurement protocols can thus monitor photoprocesses occurring in zeolite cavities with femtosecond time resolution.

Electron transfer from $[(bpy)_2RuL_{DQ}]^{4+}$ anchored on the zeolite to methylviologen in the zeolite cages has been studied on nanosecond time scale by time-resolved diffuse reflectance spectroscopy. The solid line depicting the decay of the transient signal due to $MV^{\cdot+}$ at 390 nm in Figure 3 is the simulated fit using three processes: BET, electron hopping and electron recombination, with rate constants $k_b = 9 \times 10^4 \text{ s}^{-1}$ and $k_{hop} = 6 \times 10^5 \text{ s}^{-1}$, and $k_2 = 3 \times 10^3 \text{ s}^{-1}$, respectively.

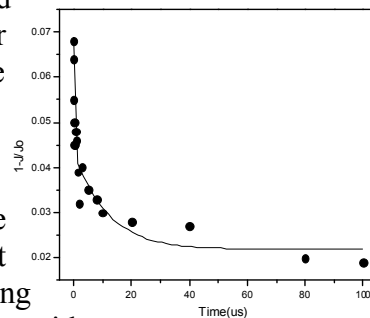


Figure 3. Decay of intrazeolitic $MV^{\cdot+}$ Upon photoexcitation of surface anchored $[(bpy)_2RuL_{DQ}]^{4+}$

IV. Hydrogen Production

Long-term hydrogen evolution via reduction of water was examined with the well known photosensitizer-acceptor system: $\text{Ru}(\text{bpy})_3^{2+}$ and methylviologen using sacrificial electron donors ethylenediamine tetra acetic acid (EDTA) and triethanolamine (TEOA) and a RuO_2 catalyst supported on zeolite Y. Online monitoring of H_2 in a continuous flow system provided information on the kinetics of H_2 production which led to the discovery that reduction of $\text{Ru}(\text{IV})$ oxide to lower valent ruthenium species is necessary for forming the active catalyst in the H_2 evolution process.

An integrated zeolite membrane on a RuO_2 containing alumina support was examined. Upon visible light illumination of $\text{Ru}(\text{bpy})_3^{2+}$, N, N¹-trimethyl-2, 2¹-bipyridinium and EDTA on the zeolite side of the membrane, charge is propagated through the zeolite membrane and transferred to propylviologen sulfonate within the pores of the alumina support. Nanofingers of ruthenium oxide was assembled within the alumina support by thermal decomposition of ruthenium dodecacarbonyl followed by oxidation of the metal. Hydrogen evolution was observed on the alumina side as visible light illumination is incident on the zeolite side of the membrane.

Future Directions :

Over the next year, growth of defect-free zeolite L membranes using the strategy shown in Figure 1 will be completed. Charge transport thorough oriented zeolite L membranes using surface anchored $[(\text{bpy})_2\text{RuL}_{\text{DQ}}]^{4+}$ and intrazeolitic bipyridinium ions will be examined. Transient spectroscopic studies in the fs-ps regime will focus on dynamics of excited-state electron delocalization in $[(\text{bpy})_2\text{RuL}_{\text{DQ}}]^{4+}$ and electron transfer to bipyridinium ions in solution and zeolites. Nanometer-sized zeolites which minimize scattering and can be investigated with transmission measurements will be used as supports. Nanosecond time-resolved diffuse reflectance studies focusing on the back electron transfer will continue on the $[(\text{bpy})_2\text{RuL}_{\text{DQ}}]^{4+}$ -bipyridinium ion system in zeolite Y, and the influence of the zeolite on photoelectron transfer will be quantitatively described. The mechanism of H_2 evolution mediated by bipyridinium radical ions on supported RuO_2 will be established.

Manuscripts acknowledging this grant :

T. Kuzniatsova, Y. Kim, K. Shqau, P.K. Dutta, and H. Verweij, "Zeta-potential measurements of zeolite Y: application in homogeneous deposition of particle coatings," *Mesopor. Micropor. Mater.*, (2007), 103(1-3), 102-107.

Yanghee Kim and Prabir K. Dutta, "An Integrated Zeolite Membrane - RuO_2 Photocatalyst System for Hydrogen Production from Water" *J. Phys Chem C* (2007), 111(28), 10575-10581.

Visible-light-driven Photoreactions of $[(\text{bpy})_2\text{Ru}(\text{II})\text{L}]\text{Cl}_2$ in Aqueous Solutions (bpy = bipyridine, L = 1,2-bis(4-(4'-methyl)-2,2'-bipyridyl) ethene), *J. Phys Chem A*, (2008), 112(5), 808-817.

T. Kuzniatsova, Y. Kim, K. Shqau, P.K. Dutta, and H. Verweij, Synthesis of thin, oriented zeolite A membrane on macroporous support, accepted in *Advanced Materials*

E. Greenbaum, Barbara Evans, Yanghee Kim and Prabir K. Dutta Mechanism of Hydrogen Production by an Artificial Photosynthetic System, submitted for publication

Jeremy White, K. Shqau, P.K. Dutta, and H. Verweij Synthesis of Randomly Oriented Zeolite L Membranes with Submicron to Micron Thicknesses, accepted in *Microporous and Mesoporous Materials*